Light Metals 2012 *Edited by: Carlos E. Suarez*
TMS (The Minerals, Metals & Materials Society), 2012

Light Metals 2012

ALUMINUM REDUCTION TECHNOLOGY

Modelling I

SESSION CHAIR
Donald Ziegler
Alcoa Canada Primary Metals
Deschambault, Canada

Light Metals 2012 *Edited by: Carlos E. Suarez*
TMS (The Minerals, Metals & Materials Society), 2012

CURRENT DISTRIBUTION AND LORENTZ FIELD MODELLING USING CATHODE DESIGNS: A PARAMETRIC APPROACH

Subrat Das[1], Guy Littlefair
[1]Subrat Das et al.; Deakin University, School of Engineering, 75 Pigdons Road, Waurn Ponds, VIC 3216, Australia

Keywords: Inclined Cathode, Current Distribution, Lorentz Field

Abstract

A mathematical model of magnetohydrodynamic (MHD) effects in an aluminium cell using numerical approximation of a finite element method is presented. The model predicts the current distribution in the cell and calculates the Lorentz force from the external magnetic field in molten metal for cathode blocks with different surface inclinations.

The findings indicated that the cathode surface inclinations have significant influence on cathode current density and Lorentz field distribution in the molten metal. The results establish a trend for the current density and associated MHD force distributions with increase in cathode inclination angle, φ. It has been found that cathode with $\varphi = 5^{o}$ inclination could decrease 16 to 20 % of Lorentz force in the molten metal.

Introduction

Worldwide, large commercial aluminium cells are being developed with capacities ranging from 300 to 500 kA. The aluminium industry is constantly searching for ways to maximize productivity and efficiency while reducing energy requirements and costs. In a typical Hall-Héroult cell, intense magnetic fields (B) are generated due to very high current in the busbars. These fields interact with the current density vectors (J) flowing in the molten metal pool within the cell, to generate magneto-hydrodynamics (MHD) forces [1, 2]. This is the basis of the instability mechanism known as metal-pad roll and interface deformation (heave), that has been extensively studied theoretically [3-6]. It is widely understood that the flow field, metal-pad heave, wave mode and degree of instability are all affected by the shape and magnitude of the magnetic field. This is why the bulk of the work has been focused on magnetic compensation through optimizing current distribution in the external bus. Very little, so far, has been done to improvise the current distribution within the cell, although, it has similar impact on the cell MHD force distribution and which is given as:

$$F = J \times B \qquad (1)$$

Where J is current distribution within the cell. The horizontal component of the current density vector J_y has a destabilizing effect. The greater the J_y, the larger is the Lorentz force, F. Figure 1 shows a typical Hall-Héroult cell where current is fed vertically through the anode, electrolyte (bath), molten aluminium, cathode blocks and bled horizontally using collector bars to the nearest external bus. The electrical conductivity of cathode is so poor relative to the aluminium metal pad that the outer third of the collector bar and cathode, nearest the sidewall of the cell, carries the most of the current load, thereby creating a very uneven cathode current distribution within the cathode. Very little current is carried into the part of the collector bar near the middle of the cell. Several researchers have reported the current distribution patterns in the aluminum reduction cell. The impacts of collector bar and inclined sidewall have been studied thoroughly. Tarapore [7] determined the horizontal current in the metal by measuring the current in steel collector bars. Fraser [8] reported the existence of current gradients due to ledge thickness.

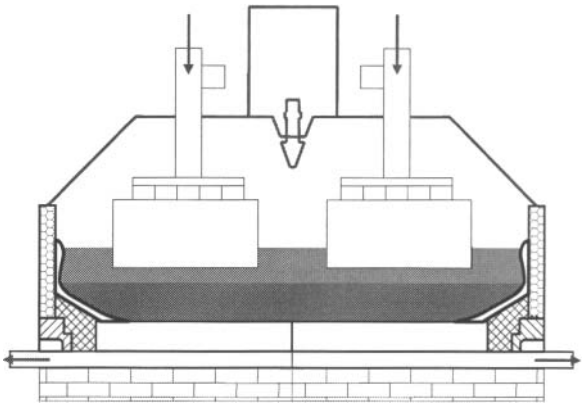

Figure 1 Schematic representation of a Hall-Héroult cell.

There have been also significant advances in the materials, design, and fabrication of cathodes in recent times. The change from anthracitic carbon to graphitized materials in cathode blocks has led to improved thermal and electrical properties and thereby the cell life. However, the graphite blocks erode more rapidly, which draws much attention in regards to higher erosion and uneven wear of cathode surface [9, 10] at higher line amperage. The erosion depths have been found to vary greatly within cathodes. These complex erosion patterns indicate that a more interrelated mechanism is involved rather than just a simplistic abrasion mechanism [11]. Several cathode autopsies reveal that wear is found to be more severe in the region with higher velocity gradient of turbulent regions [12, 13] i.e. a region where current densities are relatively higher. The wear rate decreases with increasing height of the metal pad and improved magnetic compensation. Unpublished autopsies of cells with both graphite and anthracite blocks found significant differences in wear rates, with the graphitized blocks wearing two to three times faster [12]. The wear is not even and usually found close to the region of highest metal velocities. Lombard et al [13] reported that the maximal erosion area systematically occurs at the block ends, under the anodes, known as "W shape" erosion. A thorough study of cell Lorentz field distribution led to the conclusion that there is

still a large possibility of improving the interaction of the magnetic field with the local current density in the liquid metal by modifying the cell lining design [14]. New cathode designs have shown real improvement in the cell voltage and metal pad current distribution. New cathode shapes allow decreasing the ACD without reaching the magneto-hydrodynamic instabilities[15, 16].

In this work, an inclined cathode surface is considered to allow a deeper pool in the central region to improve the current distribution. The inclination angle, φ, of the cathode surface is varied from 0 to 5°. Changing the cathode geometry and conductivity will lead to new current distribution inside the liquid metal. The objective is to evaluate the change in current distribution and Lorentz force distribution with the change in cathode surface inclinations.

CAD Model

In this study, an end-riser cell having longitudinal and transverse axes is considered. These cells are arranged transversely in rows with the electric current being passed from the cathode of an upstream (US) cell to the anode of the cell next downstream (DS). Only the half of the cell is used to predict the current distribution as shown in the figure 2 (a). All anodes share the line current (300 kA) equally. The cell has 18 anodes and 17 cathodes configuration. Cathodes are connected in parallel to carry approximately same current. Other assumptions that are:

1. Current split between US and DS cathode bus are equal;
2. Current applied to each anode are equal;
3. Resistive heating is not considered;
4. Current induction in molten metal due to the magnetic field is negligible;
5. Results are predicted for steady state condition;

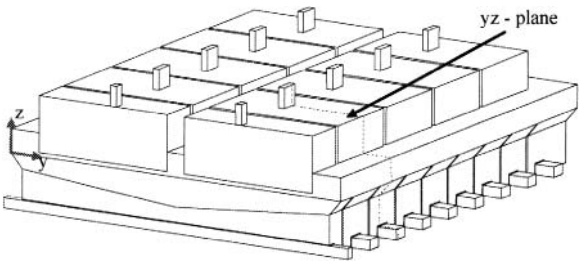

(a) 3D CAD model of one half of the cell.

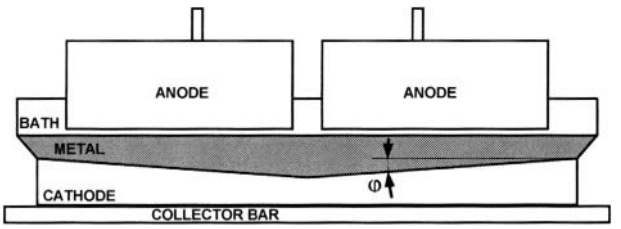

(b) Cathode shape at φ = 5°

Figure 2 CAD Model

A typical configuration of cathode surface inclination is shown in Figure 2 (b). The model uses an magnetic field (B_x, B_y, and B_z) from the parent *magnetic busbar model* to evaluate Lorentz field in the molten aluminium [14]. Thus the governing equations that used in this work are Maxwell's relations and given as:

Faraday's Law

$$\nabla \times E = -\partial B/\partial t \tag{2}$$

Ampere's Law

$$\nabla \times H = J \tag{3}$$

$$\nabla \times B = 0 \tag{4}$$

The charge conservation is

$$\nabla \cdot J = 0 \tag{5}$$

where the vector field variables are the electric field intensity, E, the magnetic field intensity, H, the magnetic flux density, B and the current density, J.

The required constitutive relations for the materials are:

$$B = \mu.H \quad \text{or} \quad H = \vartheta.B \quad \text{and} \quad J = \sigma.E \tag{6}$$

where μ is the permeability, ϑ is the reluctivity and σ is the conductivity.

The Lorentz force is then evaluated as a vector cross product of the current vector and the magnetic flux density vector in the molten metal using following relation.

$$F_x = J_y \cdot B_z - J_z \cdot B_y \tag{7}$$

$$F_y = J_z \cdot B_x - J_x \cdot B_z \tag{8}$$

$$F_z = J_x \cdot B_y - J_y \cdot B_x \tag{9}$$

$$F_n = \sqrt{F_x^2 + F_y^2 + F_z^2} \tag{10}$$

Initially, the magnetic field B_x, B_y, and B_z are computed at 300 kA line current using our *magnetic busbar model.* Subrat et al. in their recent work[14] had reported a complete 3D busbar model for the same cell considered here. The model used the parts of the cathode-bus of the upstream and downstream cells to include the magnetic field from the neighboring cells. It is to be noted that the current induction due to the moving fluid under a magnetic field will not change our results as we are predicting the difference between various models. Thus, the current induction in the molten metal due to the external magnetic field is neglected, which allows to decouple the magnetic induction and the magnetic line closure relationships. The details cell dimension and other parameters are given in the table 1.

Table 1. Cell Parameters (Base-case, $\varphi = 0^{\circ}$)

Anode Dimension (in mm)	1400 x 804 x 550
Cathode Dimension (in mm)	3348 x 447 x 400
Collector Bar (Cross-Section in mm)	150 x 100
Metal Height (in mm)	142
Cryolite Height (in mm)	228
Sidewall Channel Gap (in mm)	300
Line Current (kA)	300
Thermal Conductivity Steel (S/m)	1.031e6
Thermal Conductivity Copper (S/m)	5.998e7

Results and Discussion

A total number of 132486 tetrahedral elements were used with different meshing configurations of non-uniformly distributed gridlines. Fine grids were located in the regions near the contact zone. A grid independence test was also carried out using a higher number of elements. The present grid is found to be adequate. Results are obtained for 300 kA line current and at different inclinations of cathode surface ($0^{\circ} < \varphi < 5^{\circ}$). φ equals to 0° corresponds to horizontal cathode. The Lorentz field is evaluated using the external magnetic field (B_x, B_y, B_z) through the equations described in 7-10. The metal-pad deformation is also evaluated using Navier-Stokes equation only for the base-case model, where $\varphi = 0^{\circ}$.

Figure 3(a) shows the vector plot of current density in the typical yz plane (as indicated in Fig. 2a) for $\varphi = 0^{\circ}$. In the figure, current is only in the cryolite, metal and cathode. It is apparent from the figure that outer third of cathode carries most of the current load, which is mainly attributed to the least resistance path the cathode-collector-bar assembly. Figure 3 (b) plots the equipotential lines and the pathlines for the current density in the same yz plane. Current flows relatively vertically in the cryolite due to high electrical conductivity of the molten metal. However, in molten metal, it is apparent that the horizontal components of the current are larger. The directions of current in molten metal mostly depend upon the collector-bar output position and the least resistance path between metal and collector-bar output. However, a slightly inclined cathode surface (as shown in Fig. 2b) would increase the electrical conductivity in the central part of the cell and may flatten the current peaks on the cathode surface.

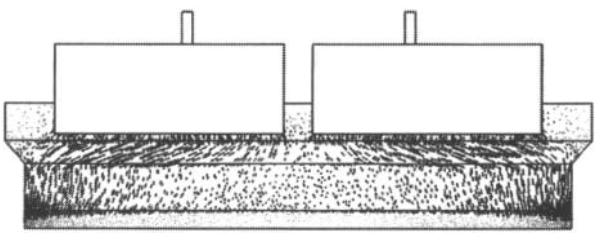

(a) Vector plot of the current density.

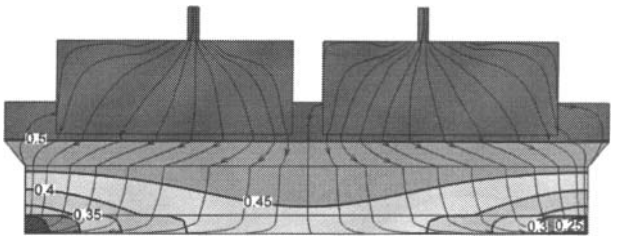

(b) Current distribution and contour of equipotential line (V) along the yz transverse plane.

Figure 3 Current Distribution

Figure 4 shows streamtracers of magnetic and vector fields of Lorentz force on the metal pad (xy plane) in one half of the cell. The lines of magnetic and Lorentz fields are orthogonal to each other. The strong rotary magnetic field shown within the cell is attributed to the vertical current in the lining and electrolyte. The Lorentz force is predicted to be toward the centre of the cell (Figure 4) resulting more static pressure in the central part of the cell, which is one of the contributing factor towards the heave formation in the aluminium cell [14]. However, the magnitude of the Lorentz force ($F = JB\,sin\theta$) in the cryolite is less due to the current direction (θ) in the cryolite.

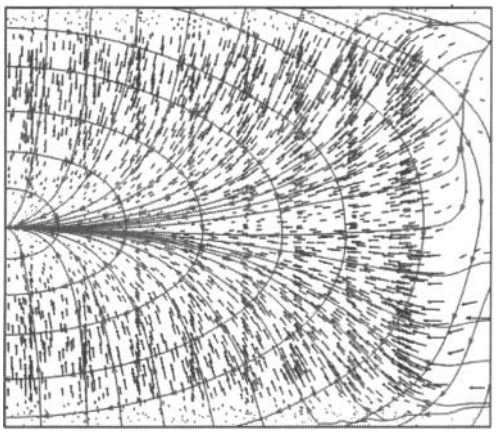

Figure 4. (a) Vector plot Lorentz field (b) streamtracers of Lorentz (red) and magnetic field.

The pressure head is calculated using the following relation [14]:

$$h_{Heave} = \frac{p}{g(\rho_{Al} - \rho_{Cryolite})} \qquad (11)$$

Moreau and Evans [17] also expressed the interface-equation in terms of difference in potential energy across the interface. Figure 5 shows the deformation of the metal pad in terms of pressure head (Heave) in the cell. Similar results are also presented by several authors [18-20].

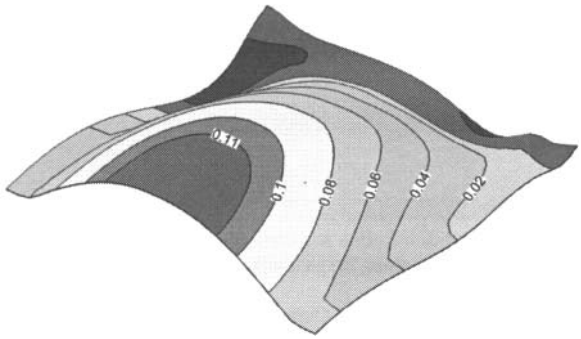

Figure 5 The metal-pad deformation (m)

Figure 6 shows the magnitude of horizontal current (J_y) and the total current along the y-axis (from the cell centre to downstream sidewall) for different inclinations of cathode surface. Horizontal current (J_y) shows a varying trend; gradually increases from the central channel to a maximum point and then down to a negative value near the sidewall. The negative current density indicates the change of direction of the current in the side channel which is due to the inclined sidewall/ledge. Xiquan et al. [13, 21] reported similar current distribution in the molten metal. In general, the peak value of current density decreases with the increase of cathode inclination. Inclined cathode allows more molten aluminium in the central channel and pushes current more towards the central part of cathode. In this way, the current gets redistributed over the cathode surface and flattens the peak current density on the cathode surface. It is apparent from the figure that a 1° change in inclination would decrease approximately 6 to 7 percent of total current density. The horizontal current density also decreases at a similar magnitude.

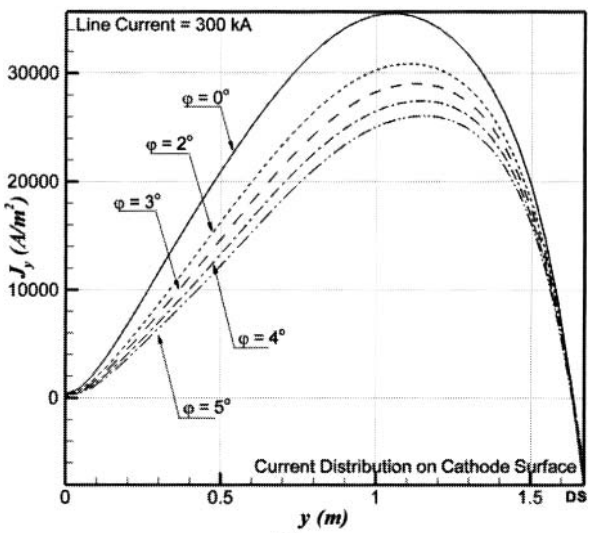

(a)

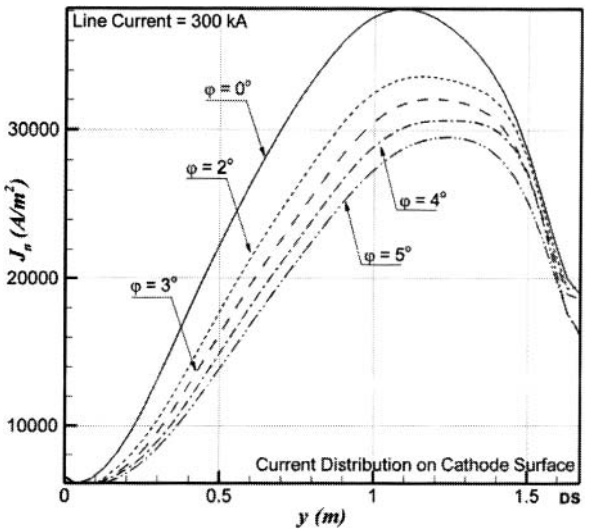

(b)

Figure 6 Current Distribution along the cathode surface (a) Horizontal (b) Nominal Current densities.

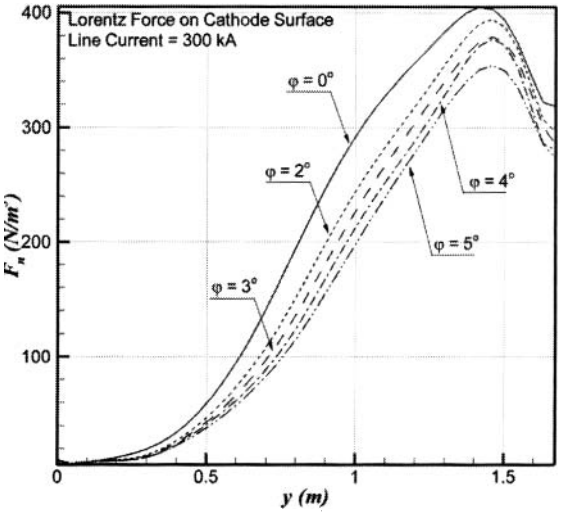

Figure 7 Lorentz Field ($F_n = \sqrt{F_x^2 + F_y^2}$)

Figure 7 shows the magnitude of Lorentz force along the cathode surface. The maximum F_n is predicted towards the sidewall of the cathode. Vector plot of Lorentz force on the metal-pad in Figure 4 also confirms the larger peripheral force. This force is mainly responsible for the heave formation and has the most detrimental effect on the cell operation under extreme instable conditions. However, the maximum value of Lorentz force decreases with increase in inclination. A slight inclination of the cathode surface could reduce this force by 5 percent approximately and a 5° cathode inclination (V cut) predicts almost 16 to 20 % decrease in Lorentz force.

Figure 8 shows the contour plots of Lorentz field using equation 10. The maximum forces are predicted to be underneath of the outer side of the anode. At higher line current this force will be

proportionally higher. It is shown in the figure that the magnitude (of Lorentz force) decreases with increase in cathode inclination. The slight inclination in cathode surface has a significant influence on Lorentz field distribution, which may have associated with many other localised phenomena such as shear stress and/or wear and tear. Many have [13, 22] also reported that the erosion phenomena is complex and attributed to several factors such as alumina abrasion, chemical attack and metal velocity. However, in this work, it is predicted that the metal velocity can be lowered using inclined anode. The maximum Lorentz force occurs at the end of the cathode block and under the outer side of the anodes (Fig 8a). Inclined cathode would decrease the Lorentz force and thereby may have some impact on metal velocity in general.

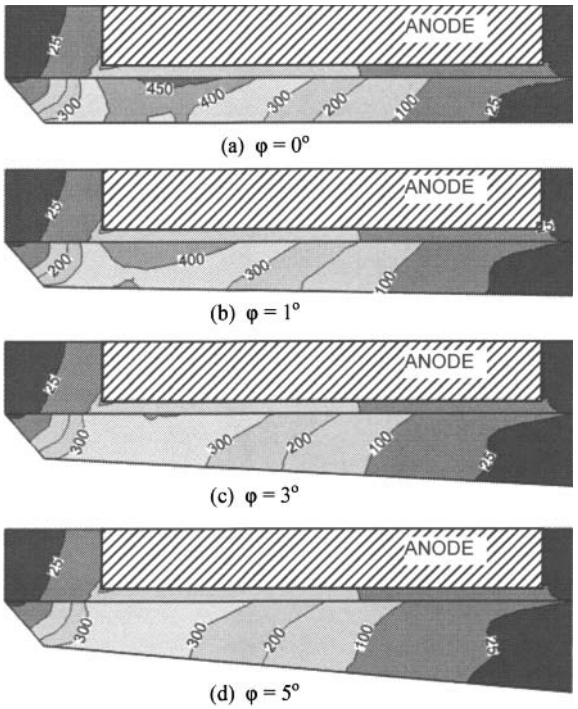

Figure 8 Contour of Lorentz Field (F_n in N/m^3) in yz plane at different cathode inclinations.

Conclusions

A 3D CAD model for one half of the cell was developed and successfully solved for Lorentz forces using external magnetic field. In this work, it has been shown that a slight inclination of the cathode surface could change the magnitude and direction of horizontal current and consequently could change the Lorentz force distribution. The force distribution along the cathode surface is clearly an indication of strong interplay among MHD forces, the geometry, and current distribution.

References

1. T. Sele, "Instabilities of the metal surface in electrolytic alumina reduction cells," *Metallurgical Transactions B,* 8(4) (1977), 613-618.
2. N. Urata, "Magnetics and Metal Pad Instability. in Light Metals: Proceedings of Sessions," AIME Annual Meeting (Warrendale, Pennsylvania) 1985.
3. A.D. Sneyd, "Stability of Fluid Layers Carrying a Normal Electric Current," *Journal of Fluid Mechanics*, 156 (1985) 223-236.
4. A.D. Sneyd, and A. Wang, "Interfacial instability due to MHD mode coupling in aluminum reduction cells," *Journal of Fluid Mechanics,* 263 (1994), 343-359.
5. D.P. Ziegler, "Stability of metal/electrolyte interface in Hall-Heì□roult cells: Effect of the steady velocity," *Metallurgical Transactions B*, 24(5) (1993), 899-906.
6. D. Billinghurst, et al., "Development of B32 cell technology," *TMS Light Metals,* (2006), 255-257.
7. E.D. Tarapore, "Effect of Some Operating Variables on Flow in Aluminum Reduction Cells," *Journal of Metals*, 34(2) (1982), 50-55.
8. K.J. Fraser, et al., "Some applications of mathematical modelling of electric current distributions in Hall Heroult cells," TMS *Light Metals, (*1989), 219-226.
9. K. Vasshaug, et al., "Formation and dissolution of aluminium carbide in cathode blocks," *TMS Light Metals*, (2009), 1111-1116.
10. Y. Sato, P. Patel, and P. Lavoie, "Erosion measurements of high density cathode block samples through laboratory electrolysis with rotation," *TMS Light Metals*, 2010, 817-822.
11. A.T. Tabereaux, et al., "Erosion of cathode blocks in 180 kA prebake cells," *TMS Light Metals,* (1999), 187-192.
12. H.A. Oye and B.J. Welch, "Cathode performance: The influence of design, operations, and operating conditions," *JOM,* 50(2) (1998), 18-23.
13. D. Lombard, et al., "Aluminum Pechiney experience with graphitized cathode blocks," *TMS Light Metals,* (1998), 653-658.
14. S. Das, G. Brooks and Y. Morsi, "Theoretical Investigation of the Inclined Sidewall Design on Magnetohydrodynamic (MHD) Forces in an Aluminum Electrolytic Cell," *Metallurgical and Materials Transactions B,* 42(1) (2011), 243-253.
15. Z. Wang, et al., "Study of surface oscillation of liquid aluminum in 168kA aluminum reduction cells with a new type of cathode design," *TMS Light Metals*, (2010), 485-488.
16. R. Von Kaenel and J. Antille, "Modeling of energy saving by using cathode design and inserts," *TMS Light Metals*, (2011), 569-574.
17. R. Moreau, and J.W. Evans, "Analysis of the Hydrodynamics of Aluminum Reduction Cells," *Journal of the Electrochemical Society*, 131(10) (1984), 2251-2259.
18. M.A. Doheim, et al., "Modeling and measurements of metal pad velocity in 208 kA end to end prebaked cells," *TMS Light Metals*, (2008), 419-424.
19. A. Moraru and A. Panaitescu. "Navier-stokes equations in presence of laplace forces in the aluminum reduction cell," *TMS Light Metals*, (2006), 521-626.
20. D.S. Severo, et al.. "Comparison of various methods for modeling the metal-bath interface," *TMS Light Metals*, (2008), 413-418.
21. Q. Xiquan, et al., "Study of current distribution in the metal pad of aluminum reduction cells," *TMS Light Metals*, (2009), 575-580.
22. S. Wilkening, and P. Reny, "Erosion rate testing of graphite cathode materials," T*MS Light Metals*, (2004), 597-602.